Technical Report
CDP-TR· 4

FACILITY FORM 602

N68-19069
(ACCESSION NUMBER) (THRU)

56
(PAGES) (CODE)

CI-86038 07
(NASA CR OR TMX OR AD NUMBER) (CATEGORY)

A FEASIBILITY STUDY OF SIGNAL PROCESSING TO IMPROVE ANTENNA GAIN

GPO PRICE $ _____

CFSTI PRICE(S) $ _____

Hard copy (HC) _3.00_

Microfiche (MF) _.65_

ff 653 July 65

MAR 1968
RECEIVED
NASA STI FACILITY
INPUT BRANCH

RAYTHEON COMPANY · EQUIPMENT DIVISION
communications and data processing operation RAYTHEON

A FEASIBILITY STUDY OF SIGNAL PROCESSING
TO IMPROVE ANTENNA GAIN

Technical Report No. CDP-TR-4
by
R. G. Cease
C. K. H. Tsao
W. J. Bickford
and
H. J. Rowland

FINAL REPORT
November 1967

Prepared for

Electronics Research Center
National Aeronautics and Space Administration
Cambridge, Massachusetts

under

Contract No. NAS 12-529

RAYTHEON COMPANY
Equipment Division
Communications and Data Processing Operation
Norwood, Massachusetts 02062

CONTENTS

LIST OF ILLUSTRATIONS

ABSTRACT

A signal processor, employing a synthetic phase isolator (SPI), has been investigated analytically and experimentally for application in an adaptive antenna array which is illuminated simultaneously by a coherent signal source and a partially coherent interfering source. The performance of the signal processing array is discussed in terms of processing gain and tracking error.

It is shown that, when the partially coherent interfering source has large angular extent relative to the theoretical plane wave beamwidth of the antenna array, large processing gain is achieved. For a nearly coherent interfering source, the performance of the array exhibits a "capturing effect" as in an FM receiver. That is, the adaptive array tends to form a beam in the direction of the stronger of the two sources. The amount of discrimination against the weaker source depends on, but not entirely, the "pattern factor" of the array.

Numerical examples are shown for a four-element linear array.

i

I. INTRODUCTION

The theory and experimental results of the SPI signal processor have been presented previously by Bickford, Cease, Cooper and Rowland [1]. The signal processor consists of N identical synthetic phase isolators (SPI), each of which processes the signal from a corresponding antenna element of the array, and a combiner which sums the output of the SPI's. As shown by Bickford et al, this signal processor results in maximal ratio combining [2, 3] and has application in predetection diversity combining in communications systems as well as in adaptive phasing of a large antenna array.

It is frequently necessary to employ an antenna array to receive radiation from a desired source under the condition of interference from background radiation from radio astronomical sources. In radio communications, the desired source is normally a coherent point source, while the background radiation is classified as partially coherent. In this report, we examine the effect of partially coherent radiation on the output of a phased array and analyze the performance of the array in conjunction with an SPI signal processor.

II. THEORY OF OPERATION

A. SPI Signal Processor

We consider an N-element antenna array. The array elements have output voltage v_{a_i}, $i = 1, 2, \ldots, N$. In a normal phased array, these antenna voltages are passed through phasing networks prior to combining. The purpose of the phasing networks is to form a beam in a desired direction in space. To form a beam adaptively, i.e. in the direction of the signal source no matter what the direction may be, a signal processor is used.

1

The signal processor must compensate the retardation phase of each antenna voltage.* In the SPI signal processor, this is accomplished in the manner shown in Figure 1. The operation is as follows. The output of the combiner $v_0(t)$ is applied to the first mixer of the ith SPI channel where it is multiplied with input v_{a_i} to result in

$$v_{1_i}(t) = \frac{1}{2} v_{a_i}^*(t) v_0(t) \tag{1}$$

[Note - All time functions are complex low frequency envelope functions of the actual waveform, i.e. with factor $e^{j\omega t}$ suppressed. The asterisk denotes complex conjugate.]

The filter, F_1 with impulse response $f_1(t)$, has an output

$$v_{2_i}(t) = \int_0^\infty v_{1_i}(t-\tau) f_1(\tau) \, d\tau \tag{2}$$

The second mixer output is

$$v_{3_i}(t) = \frac{1}{2} v_{2_i}(t) v_{a_i}(t) \tag{3}$$

Note that the first mixer operates on the conjugate of v_{a_i} as indicated by the asterisk in Equation 1, while no conjugation is involved in the second mixer.

The outputs of the SPI's are combined,

$$v_4 = \sum_{i=1}^N v_{3_i}(t) \tag{4}$$

where N is the number of channels in the SPI signal processor.

*Implicit in this statement is the requirement that the antenna bandwidth is greater than the receiver bandwidth so that envelope delay equalization is unnecessary. This point will be touched upon in Section II-B.

2
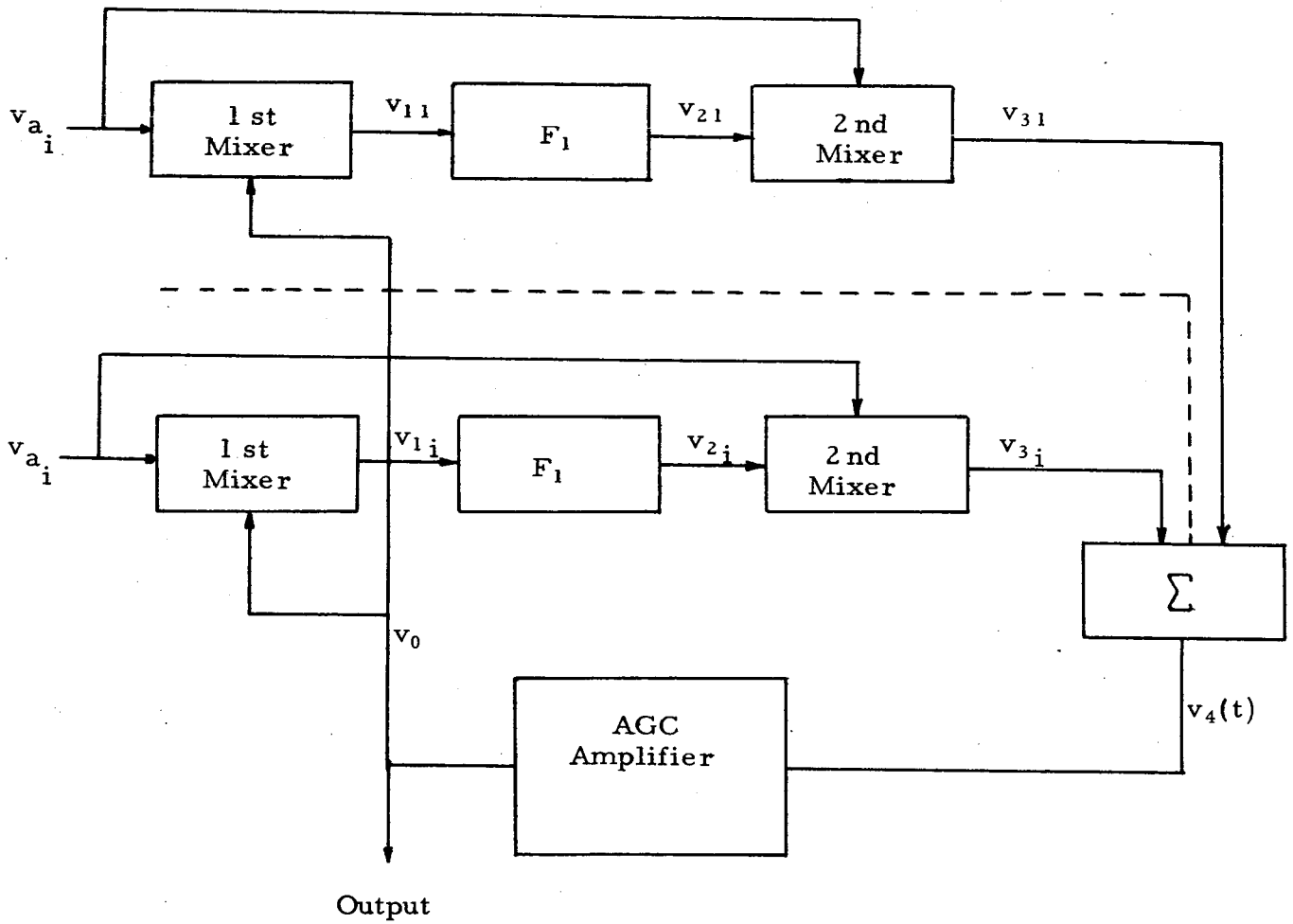
Figure 1.

Functional Block Diagram of an N-Channel SPI Signal Processor

The summer output, v_4, is applied to an AGC amplifier to result in the signal processor output

$$v_0(t) = G(t) v_4(t) = \frac{1}{2} G(t) \sum_{i=1}^{N} v_{2_i}(t) v_{a_i}(t) \tag{5}$$

where $G(t)$ is a positive real function of time, i. e. it is the gain of a non-inverting broadband amplifier with no time delay.

Substituting (1) in (2),

$$v_{2_i}(t) = \frac{1}{2} \int_0^\infty v_{a_i}^*(t-\tau) v_0(t-\tau) f_1(\tau) \, d\tau \tag{6}$$

If the filter F_1 is a low pass network with bandwidth

$$b \ll w \tag{7}$$

where w is the spectral width of the input, v_{a_i}, the integral in (6) is approximately the cross-correlation function of v_{a_i} and v_0, and the output of the filter is

$$v_{2_i}(t) = A_i + v_{f_i}(t) \tag{8}$$

where A_i is a complex constant and $v_{f_i}(t)$ is a low pass time function. The constant is

$$A_i = \frac{1}{2} \overline{v_{a_i}^*(t) v_0(t)} \tag{9}$$

For b sufficiently smaller than w,

$$\overline{A_i^2} \gg \overline{v_{f_i}^2} \tag{10}$$

4

and
$$v_{2_i}(t) \approx A_i \qquad\qquad (11)$$

With the assumptions in (10), we combine equations (11) and (2) through (5) and obtain

$$v_0(t) = \frac{1}{2} G(t) \sum_{i=1}^{N} A_i v_{a_i}(t) \qquad\qquad (12)$$

In the above expression, $G(t)$ represents the transmittance of the AGC amplifier and is a function of the amplitude of v_4. Earlier, we assumed that the ith filter F_1 output is a constant A_i. We may make a similar assumption with regard to the action of the AGC amplifier. That is, if the time constant of the AGC amplifier is comparable to or longer than the time constant of the filter, then within one integration time constant of the filter F_1, the filter output is constant and the AGC amplifier gain is also constant. (For a detailed discussion on the AGC time constant and filter bandwidth requirements, see Ref. [1]). Hence,

$$G(t) \approx G_0 \qquad\qquad (13)$$

These assumptions are justified if the input variables, v_{a_i}'s, are at least wide sense quasi-stationary processes over the time intervals under consideration.

With (13) and (12), we obtain from (7) and (11)

$$A_i = \frac{G_0}{4} \int_0^{\infty} v_{a_i}^*(t-\tau) \sum_{k=1}^{N} A_k v_{a_k}(t-\tau) f_1(\tau) d\tau \qquad\qquad (14)$$

Based on the earlier assumption in (9), (14) reduces to

$$A_i = \frac{G_0}{4} \int_0^{\infty} v_{a_i}^*(t) \sum_{k=1}^{N} A_k v_{a_k}(t) dt$$

$$= \frac{G_0}{4} \sum_{k=1}^{N} A_k \int_0^\infty v_{a_i}^*(t) \, v_{a_k}(t) \, dt$$

$$= \frac{G_0}{4} \sum_{k=1}^{N} A_k \, \mu_{i_k} \tag{15}$$

where $\quad \mu_{i_k} = \overline{v_{a_i}^*(t) \, v_{a_k}(t)}$ $\qquad\qquad$ (16)

is the covariance function.

We may write equation (15) in matrix notations, [4],

$$\frac{G_0}{4} [\mu_{i_k}] [A_i] - [U] [A_i] = 0 \tag{17}$$

where $[\mu_{i_k}]$ is the covariance matrix, $[A_i]$ is a column matrix, and $[U]$ is the unity matrix.

Equation (17) may be solved for A_i's. For non-trivial solutions, the characteristic function must be identically zero,

$$\frac{G_0}{4} |\mu_{i_k}| - |U| = 0 \tag{18}$$

To summarize, for an N-channel signal processor, the inputs are $v_{a_i}(t)$ with covariance function μ_{i_k} ; i, k = 1, 2, . . . , N. The output of the processor is

$$v_0(t) = \frac{1}{2} G_0 \sum_i A_i \, v_{a_i}(t)$$

where the A_i's are solutions of Equation (17).

The results cited here are based on the assumptions that the inputs are quasi-stationary processes over intervals comparable to the

time constants of the filter F_1 and the AGC amplifier and that the filter bandwidth (as well as AGC amplifier bandwidth) is sufficiently narrow to have negligible fluctuating component at its output.

B. Input Covariance Functions

The performance of the signal processor is governed by the covariance matrix of the input waveforms. We can represent the voltage waveforms from the ith element of an array as

$$v_{a_i} = v_{s_i} e^{j\phi_{s_i}} + v_{n_i} e^{j\phi_{n_i}} \tag{19}$$

where v_{s_i} and v_{n_i} are respectively the complex envelopes of the signal from a point source and noise from an extended source. The angles ϕ_{s_i} and ϕ_{n_i} are the retardation phases associated with the ith element for the signal and the noise respectively.

At this point, we need to digress for a moment and discuss the properties of partially coherent radiation. Most of the natural radiation sources, such as radio stars, are partially coherent. We shall consider a source being located at a large distance R from two points p_1 and p_2 as shown in Figure 2. p_1 and p_2 are separated by distance y transversal to the direction of the source and by distance z, longitudinal to the source, with y<<R and z<<R. The baseline separation between p_1 and p_2 is ℓ so that

$$y = \ell \cos \theta_n \tag{20}$$

$$z = \ell \sin \theta_n \tag{21}$$

where θ_n is the direction of the source measured from the normal to the baseline.
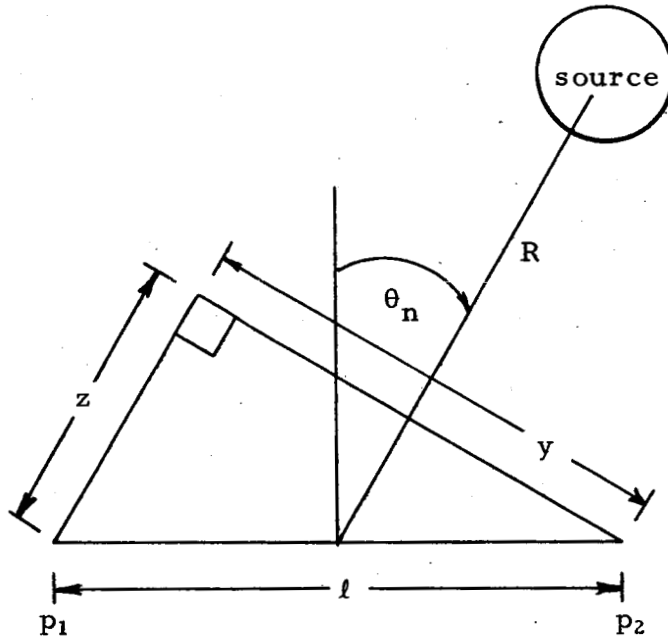
Figure 2.

Geometrical Configuration

We assume that, at points p_1 and p_2, we are restricted to view the radiation in an angular bandwidth $\Delta\omega$, centered at a mean angular frequency ω_0. The angular width extended by the source is β. With such a source, the waveforms at p_1 and p_2 are respectively,

$$v_{n_1} e^{j\phi_{n_1}} \text{ and } v_{n_1} e^{j\phi_{n_2}}$$

where ϕ_{n_1} and ϕ_{n_2} are the retardation phase angles. The correlation coefficient[5,6] of v_{n_1} and v_{n_2} is

$$\gamma_{12} = \frac{\overline{v_{n_1}^* v_{n_2}}}{\sigma_n^2} = \text{sinc}\left(\frac{\pi\beta\ell\cos\theta_n}{\lambda_0}\right)\text{sinc}\left(\frac{\Delta\omega_0\ell\cos\theta_0}{c}\right) \quad (22)$$

8

Let $\alpha = \dfrac{\sigma_n^2}{\sigma_s^2}$ (25)

$$\delta_{ik} = (\phi_{s_i} - \phi_{n_i}) - (\phi_{s_k} - \phi_{n_k})$$ (26)

$$\rho_{ik} = \alpha \gamma_{ik} \exp(j\delta_{ik})$$ (27)

We obtain by substituting Equations (25) through (27) in (24),

$$\mu_{ik} = \sigma_s^2 \exp(j\phi_{s_k} - j\phi_{s_i})\,[1 + \rho]$$ (28)

C. Eigenvector

By substituting (28) in (17) and using the new variable

$$x_i = A_i\, e^{j\phi_{s_i}}$$ (29)

we reduce Equation (17) to

$$([P] - \lambda[U])\,[X] = 0$$ (30)

where $[U]$ = unity matrix

$[X]$ = column matrix with elements x_i

$$\lambda = \frac{4}{\sigma_s^2\, G_0}$$ (31)

and $[P] = \begin{bmatrix} 1+\rho_{11}, & 1+\rho_{12}, & \ldots\ldots, & 1+\rho_{1N} \\ 1+\rho_{21}, & 1+\rho_{22}, & \ldots\ldots, & 1+\rho_{2N} \\ \ldots & \ldots & \ldots\ldots & \ldots\ldots \\ 1+\rho_{N1}, & 1+\rho_{N2}, & \ldots\ldots, & 1+\rho_{NN} \end{bmatrix}$ (32)

The set of linear equations corresponding to the matrix equation in (30) is

$$\lambda x_i = \sum_k x_k (1 + \rho_{ik}) \tag{33}$$

Note that the coherence coefficient γ_{ik} is an even function with respect to indices i and k, while the exponential factor δ_{ik} in (26) is an odd function in i and k. Thus, $\mu_{ik} = \mu_{ki}^*$ and $\rho_{ik} = \rho_{ki}^*$, and the matrices $[\mu_{ik}]$ and $[P]$ are both Hermitian.

Since Equation (30) is Hermitian, there are N eigenvalues for λ which are all real. In the present analysis, we have assumed that G_0 is positive real so that the eigenvalues obtained from Equation (30) must be positive and real. Furthermore, λ must be non-zero. Thus, it can be shown that one and only one eigenvalue comprises the desired solution as the other eigenvalues become zero under certain input environments such as for $\gamma_{ik} = 0 (i \neq k)$. Furthermore, that eigenvalue which has the highest value (corresponding to lowest value in G_0) is the desired root of Equation (30).

Corresponding to the appropriate eigenvalue λ, we obtain an eigenvector

$$X = \{x_1, x_2, \ldots, x_i, \ldots, x_n\} \tag{34}$$

where $x_i = A_i \exp(j\phi_{s_i})$

The components of the eigenvector are the output of the narrowband filter (Figure 1) multiplied by the retardation phase angle, ϕ_{s_i}, for the desired signal. The eigenvector or the characteristic vector is therefore the array weighting function.

Substituting x_i in Equation (12) and using Equation (19), (with $v_s = v_{s_i}$, i = 1, 2, . . . , N), the signal processor output becomes

11

$$v_0 = \frac{1}{2} G_0 \sum_{i=1}^{N} x_i v_s + \frac{1}{2} G_0 \sum_{i=1}^{N} x_i v_{n_i} e^{j\phi_{n_i} - j\phi_{s_i}} \tag{35}$$

In the above, the first part on the left hand side is the signal output, and the second term is the noise output, these are respectively,

$$v_{s_0} = \frac{1}{2} G_0 v_s \sum_{i=1}^{N} x_i \tag{36}$$

$$v_{n_0} = \frac{1}{2} G_0 \sum_{i=1}^{N} x_i v_{n_i} e^{j(\phi_{n_i} - \phi_{s_i})} \tag{37}$$

Equations (36) and (37) show clearly that the x_i's are the phased array weighting functions. For a uniform illumination, x_i's should have identical magnitudes. For forming a beam in the direction of the signal, the x_i's should have phase angles which are identically zero.

In the next section, we shall examine the properties of the eigenvector X.

III.   SYSTEM PERFORMANCE

A.   Weighting Functions

The linear equations in (33) can be solved for the weighting functions, x_i's, by the recurrence method [7] for limiting cases. We have from Equation (33)

$$\lambda x_i = \sum_k x_k + \sum_k x_k \rho_{ik} \tag{38}$$

By changing indices and substituting this into the second term on the right hand side of Equation (33), and repeating the process, we obtain

$$\lambda x_i = E\left[1 + \frac{1}{\lambda} T_{ik} + \frac{1}{\lambda^2} T_{ik}T_{k\ell} + \frac{1}{\lambda^3} T_{ik}T_{k\ell}T_{\ell m} + \ldots\right] \tag{39}$$

where
$$E = \sum_{k=1}^{N} x_k$$

$$T_{ik} = \alpha \sum_{k} \rho_{ik}$$

1. Incoherent Noise Source

If the noise source is incoherent,

$$T_{ik} = \sum_{k} \rho_{ik} = \alpha \tag{40}$$

and Equation (40) becomes

$$\lambda x_i = E\left[1 + \frac{\alpha}{\lambda} + \frac{\alpha^2}{\lambda^2} + \ldots\right] \tag{41}$$

$$= \frac{E\lambda}{\lambda - \alpha}$$

From this, we obtain, by summing over index i

$$\lambda_1 - \alpha = N \tag{42}$$

and
$$x_i = \frac{E}{\lambda_1 - \alpha} = \frac{E}{N} \tag{43}$$

This special case results in only one finite, non-zero eigenvalue for λ.

2. Coherent Noise Source

If the noise source is coherent, i.e. a point source, $\gamma_{ik} = 1$, we have

13

$$T_{ik} = \alpha \sum_k e^{j\delta_{ik}} = \alpha\, e^{j(\phi_{s_i} - \phi_{n_i})} \sum_k e^{-j(\phi_{s_k} - \phi_{n_k})}$$

$$= \alpha\, e^{j(\phi_{s_i} - \phi_{n_i})}\, N\, F \tag{44}$$

where
$$F = \frac{1}{N} \sum_k e^{-j(\phi_{s_k} - \phi_{n_k})} \tag{45}$$

F is the field intensity array pattern factor.

Using (44) in (40),

$$\lambda\, x_i = E\left[\, 1 + \frac{\alpha}{\lambda}\, e^{j(\phi_{s_i} - \phi_{n_i})}\, NF\left(1 + \frac{N\alpha}{\lambda} + \frac{N^2\alpha^2}{\lambda^2} + \ldots \right)\right]$$

$$= E\left[\, 1 + \frac{\alpha NF}{\lambda - \alpha N}\, e^{j(\phi_{s_i} - \phi_{n_i})}\,\right] \tag{46}$$

To solve for λ, we again take the summation of index i and obtain

$$(\lambda - N)\,(\lambda - \alpha N) = \alpha N^2\, F^* F$$

where
$$F^* = \frac{1}{N} \sum_k e^{j(\phi_{s_k} - \phi_{n_k})}$$

In accordance with the earlier discussion, the desired eigenvalue (the largest in value) is

$$\lambda_1 = \frac{1}{2} N(1 + \alpha) + \frac{1}{2} N \sqrt{(1-\alpha)^2 + 4\alpha\, FF^*} \tag{47}$$

Substituting this in (46)

$$x_i = \frac{E}{\lambda_1} \left\{ 1 + \frac{2\alpha F}{(1-\alpha)\left[1 + \sqrt{1 + \dfrac{4\alpha\, |F|^2}{(1-\alpha)^2}}\,\right]}\, e^{j(\phi_{s_i} - \phi_{n_i})} \right\} \tag{48}$$

14

3. Partially Coherent Source

For a source which is finite in extent, no general method is applicable to obtain a solution in closed form, and numerical techniques must be employed for specific situations. As an example, we consider, in Section V, a four-element, equally spaced linear array.

B. Signal Processing Gain

The signal processing gain of the array is defined as the ratio of output signal-to-noise ratio $(S/N)_{input}$. By our previous definition,

$$(S/N)_{input} = \frac{\sigma_s^2}{\sigma_n^2} = \frac{1}{\alpha}$$

The output signal and noise powers may be obtained by finding the auto-covariance of v_{s_0} and v_{n_0}. This process results in output signal power

$$S_0 = \frac{G_0^2 \sigma_s^2}{4} \sum_{i=1}^{N} \sum_{k=1}^{N} x_i x_k^*$$

and output noise power

$$N_0 = \frac{G_0^2 \sigma_n^2}{4} \sum_{i=1}^{N} \sum_{k=1}^{N} \gamma_{ik} x_i x_k^* e^{-j\delta_{ik}}$$

The processing gain is accordingly

$$\frac{S_0}{N_0} \alpha = \frac{\sum_{i=1}^{N} \sum_{k=1}^{N} x_i x_k^*}{\sum_{i=1}^{N} \sum_{k=1}^{N} \gamma_{ik} x_i x_k^* e^{-j\delta_{ik}}} \tag{49}$$

15

1. Incoherent Noise Source

The signal processing gain when viewing a signal in the presence of incoherent (uniform background) noise is

$$\frac{S_0}{N_0} \alpha \; = \; N \tag{50}$$

2. Coherent Noise Source

For interference from a coherent noise source, the signal processing gain is

$$\frac{S_0}{N_0} \alpha \; = \; \frac{1}{|F|^2} \; \frac{1-\alpha + \sqrt{(1-\alpha)^2 + 4\alpha |F|^2} + 2\alpha |F|^2}{1-\alpha + \sqrt{(1-\alpha)^2 + 4\alpha |F|^2} + 2\alpha} \tag{51}$$

We note that for

    a. $\alpha \to 0$

$$\frac{S_0}{N_0} \alpha \to \frac{1}{|F|^2}$$

    b. $\alpha = 1$

$$\frac{S_0}{N_0} \alpha = 1$$

    c. $\alpha \to \infty$

$$\frac{S_0}{N_0} \alpha \to |F|^2$$

    d. $|F|^2 = 1$

$$\frac{S_0}{N_0} \alpha \to 1$$

The processing gain is a function of the array pattern factor as well as the input signal-to-noise ratio σ_s^2/σ_n^2, as shown in

Figure 3 with $|F|^2$ as a parameter. For large signal-to-noise ratio, the "processing gain" approaches in magnitude the inverse of the array pattern factor. For very low signal-to-noise ratio, we have a "processing loss" of an amount equal to the pattern factor. Thus the signal processing array always enhances the stronger of the two signals. This phenomenon is similar to the "capture effect" in an FM receiver.

C. Effect on a Modulated Signal

As shown in Section II-C, the signal processor output is, for the signal component,

$$v_{s_0} = \frac{1}{2} G_0 \, v_s \sum_{i=1}^{N} x_i \tag{52}$$

Since we have stipulated that the narrowband filter has a bandwidth sufficiently narrow in comparison with the bandwidth of the receiver and that the inputs to the antennas are statistically stationary, the x_i's can be assumed constant. Thus, Equation (52) indicates that the signal processing antenna array reproduces the signal with its modulation faithfully without distortion.

D. Effect of Both Uniform and Extended Noise Sources

The objective of this study is to consider an array operated under the following environments.

1. A coherent source is viewed against uniform sky noise,

2. A coherent source is viewed against an extended noise source as well as uniform sky noise,

3. A coherent source is viewed against a uniform background noise as well as in the presence of a discrete interference source.
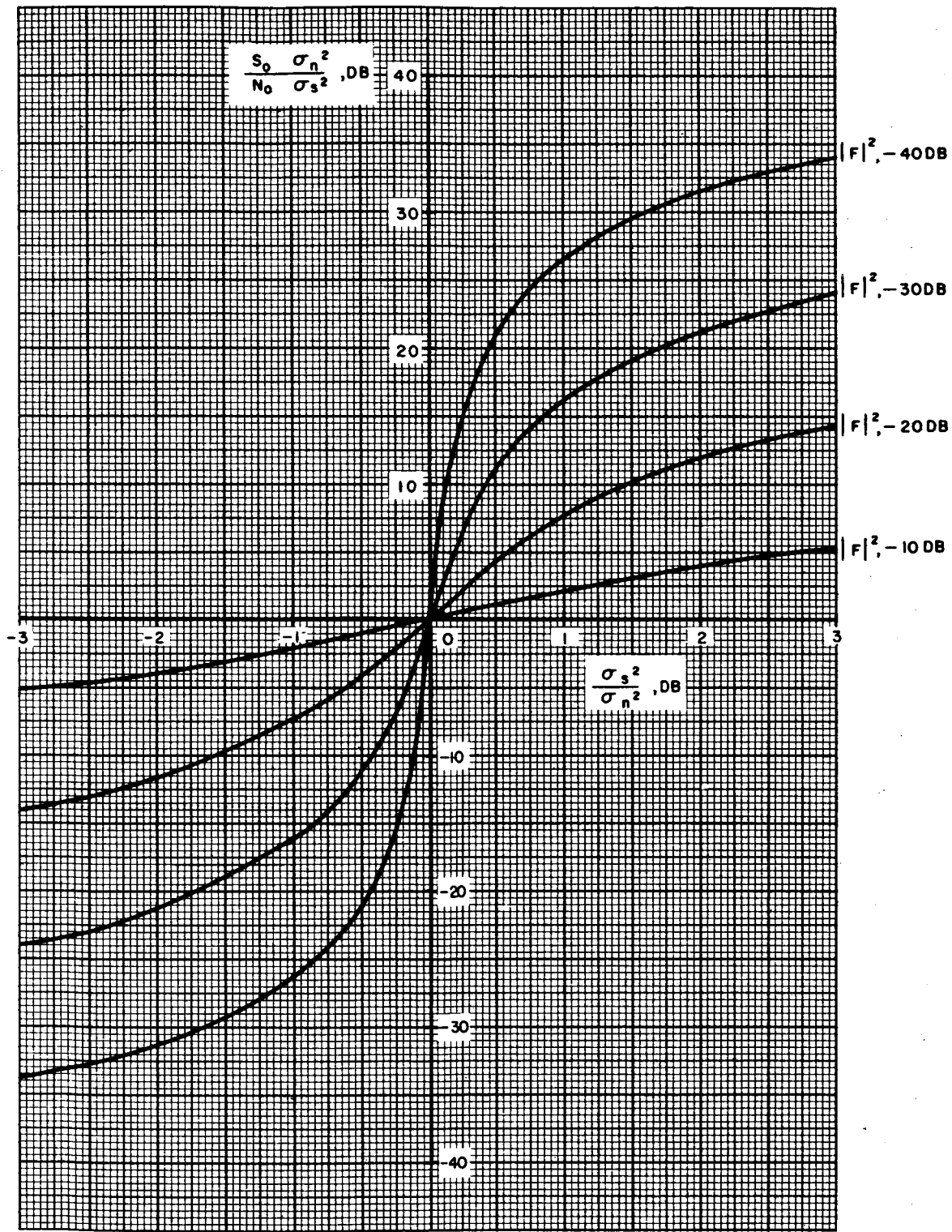
Figure 3.   Signal Processing Gain as Function of Input Signal-
to-Noise Ratio for Noise from a Point Source

The analysis of the signal processor has been carried out on the basis of viewing a coherent signal in the presence of an extended noise source. This analysis is readily specialized for Case 1 above by requiring β to be large (or $\gamma_{ik} = 0$ for $i \neq k$).

The requirement in Case 2 above can be met by the following consideration. If the noise is from two extended sources, the noise voltage from the antenna is

$$v_{n_i} = v_{x_i} \exp(j\phi_{x_i}) + v_{y_i} \exp(j\phi_{y_i}) \tag{53}$$

where the subscripts x and y identify the contribution from sources x and y, respectively.

We assume $\overline{v_{x_i}^* v_{x_i}} = \sigma_x^2$ and $\overline{v_{y_i}^* v_{y_i}} = \sigma_y^2$ for $i = 1, 2,$ . . . , N. Then the variance of v_{n_i} is

$$\overline{v_{n_i}^* v_{n_i}} = \sigma_x^2 + \sigma_y^2 \tag{54}$$

where it is assumed that the radiations from the sources x and y are uncorrelated.

The covariance corresponding to the ith and k^{th} elements is

$$\overline{v_{n_i}^* v_{n_k}} = \overline{v_{x_i}^* v_{x_k}} \, e^{-j\phi_{x_i}} e^{j\phi_{x_k}} +$$

$$\overline{v_{y_i}^* v_{y_k}} \, e^{-j\phi_{y_i}} e^{j\phi_{y_k}} \tag{55}$$

We identify y as the uniform sky noise so that

$$\overline{v_{y_i}^* v_{y_k}} = 0 \qquad \text{for } i \neq k$$
$$= 1 \qquad \text{for } i = k \tag{56}$$

and identify x as the extended source with

$$\overline{v_{x_i}^* v_{x_k}} = \gamma_{x_{ik}} \sigma_x^2 \tag{57}$$

where $\gamma_{x_{ik}} = 1$, for $i = k$ (58)

Substituting (57) and (56) in (55)

$$\overline{v_{n_i}^* v_{n_k}} = \sigma_x^2 \left(1 + \frac{\sigma_y^2}{\sigma_x^2}\right), \quad \text{for } i = k$$

$$= \sigma_x^2 \gamma_{x_{ik}} e^{-j\phi_{x_i}} e^{j\phi_{x_k}}, \quad \text{for } i \neq k \tag{59}$$

Comparing (59) with the coherence coefficient for an extended source, we conclude that the requirements of Case 2 are immediately taken care of by modifying the coherence coefficients:

$$\gamma_{ii} \rightarrow 1 + \frac{\sigma_y^2}{\sigma_x^2} \tag{60}$$

Similar modifications apply in Case 3 where the extended source is now in its limiting form, namely a discrete source.

IV. DISCUSSION

The analysis above has been based on a steady state situation. The general behavior of the signal processor will be discussed below in a heuristic manner, particularly with regard to the presence of two point sources.

In our approach, we have regarded the signal processor as a device which determines the input phase retardation angles associated with each input and produces the correct weighting factors, i. e. A_i's and the corresponding x_i's, to compensate for these phase angles so

that the resultant waveforms can be combined in phase. This is found
to be so if the array is illuminated by a coherent source in the presence
of an incoherent (extended) source. Because of this property, the sig-
nal voltages always add in phase, while the noise from each channel
would add on a power basis. Hence, there is a processing gain equal
to N, the number of elements. This is so regardless of the input signal-
to-noise ratio, nor does it depend on the array configuration. Implicit
in this conclusion is the fact that many noise sources can be viewed as
being incoherent only if the array spacings are sufficiently large (see
Equation 22).

The situation where both the signal and the noise (or inter-
ference) are due to point sources is less straightforward. Intuitively,
one may predict that, if the interference level is much weaker than the
signal level, the signal processor will be controlled by the strong signal.
Simultaneous to this, one predicts that the interference or noise voltages
from each SPI channel will add on a voltage basis rather than a power
basis because of the point source assumption. Hence we will not have a
processing gain equal to N. On the other hand, because of the retarda-
tion phase angles relative to those for the signal voltages, the noise
voltages combine by the usual rule governing the array radiation pattern.
Thus, if we consider that the array is phased to have the main beam
pointed in the direction of the signal, the noise output power will be re-
duced by a factor of $|F|^2$ relative to the output signal power, $|F|^2$ being
the normalized array power pattern. The same discrimination applies to
the signal if it is weaker than the noise, as the main beam will then be
directed to the coherent noise source. It is realized that this is an over-
simplified picture.

The signal processing gain (or loss, for that matter) is
strongly influenced by the input signal-to-noise ratio. Furthermore, it
is a function of the array configuration as reflected in the "pattern factor"
F. Thus, if either the input signal-to-noise ratio or the "pattern factor"

F, defined in Equation (45), is unity, the signal processing gain is 0 db. This situation may be looked upon as though the main beam were directed toward the point half way between the directions of the signal and noise sources. This is, in fact, not so, and there lies the principal difference between the nature of the SPI signal processing array and the conventional adaptive phased array.

We recall that

$$x_i = a[1 + D^2 e^{j(\phi_{s_i} - \phi_{n_i})}] \tag{61}$$

where

$$a = \frac{E}{\lambda_1} = \frac{1}{\lambda_1} \sum_k x_k$$

and

$$D^2 = \frac{2\alpha F}{1 - \alpha + \sqrt{(1-\alpha)^2 + 4\alpha |F|^2}} \tag{62}$$

We note that x_i is a complex quantity in which both amplitude and phase are functions of the input signal-to-noise ratio, the array configuration, and the relative directions of arrival $\phi_{s_i} - \phi_{n_i}$. Whereas in normal phased arrays each array element channel has the same gain, the SPI signal processing array has unequal gain which may indeed be zero under special circumstances. This condition is due to the ratio-square characteristics of the signal processor.

To further appreciate the behavior of the signal processor under conditions of excitation by two point sources, we obtain, from Equations (29) and (61),

$$A_i = b(\frac{1}{D} e^{-j\phi_{s_i}} + D e^{-j\phi_i}) \tag{63}$$

where

$$b = \frac{E}{\lambda_1} D$$

We further note that the output signal and noise components are, respectively,

$$v_{s_0} = \frac{G_0}{2} \sum_i A_i v_s e^{j\phi_{s_i}} = Cv_s \left(\frac{1}{D} + DF^*\right) \tag{64}$$

$$v_{n_0} = \frac{G_0}{2} \sum_i A_i v_{n_i} e^{j\phi_{n_i}} = Cv_n \left(\frac{F}{D} + D\right) \tag{65}$$

where $\qquad C = \frac{G_0}{2} bN$

and $\qquad v_n = v_{n_i}$ for a coherent noise source.

Equations (64) and (65) show that the signal processing array forms effectively two beams. One beam with voltage gain $\frac{1}{D}$ is in the direction of the signal source, while the second beam with voltage gain D is in the direction of the source. The magnitudes $\frac{1}{D}$ and D are the weighting factors for the two beams. For a large signal, $\frac{1}{D} \gg 1$ so that only the beam directed to the signal source is effective, while for a relatively weak signal (strong noise) $D \gg 1$ and the second beam becomes the contributing factor on the signal processor output. For equal signal and noise power at the input, the two beams have equal gain and the processor has a signal processing gain of unity.

It should be quite evident from Equations (64 & 65) that for signal and noise sources in such directions that F = 0, we have a degenerate case with

$$v_{s_0} = \frac{D}{S} = \frac{Cv_s}{D}.$$

$$v_{n_0} = Cv_n = Cv_n D$$

This situation arises because the beam pointed toward the signal has a null, i.e. F = 0, in the direction of the noise, and vice versa. Under

this condition, the signal processing gain is either infinite (for $\sigma_s^2 > \sigma_n^2$), zero (for $\sigma_s^2 < \sigma_n^2$) or unity (for $\sigma_s^2 = \sigma_n^2$). The transition is theoretically a step function.

Let us assume that the source A is turned on and source B is turned off. In the direction of A, we have formed the Beam A. This beam has a null in the direction of B. Now we turn on source B at time $t = 0$. The signal processor has a set of weighting functions x_i's which form a beam with a null in the direction of B at $t = 0-$. The combiner output does not contain a component due to source B at time $t = 0+$. Furthermore, since the two sources are not correlated, the weighting functions x_i's do not change. Thus, it appears that the system would not respond to source B, even though this source may be much stronger than source A. This would seem to contradict the result of the steady state analysis that, if B is stronger than A, the beam in the direction of B should be the dominant one.

The above contradiction is readily resolved in favor of the steady state analysis by the fact that the signal processor is a regenerative device. Prior to turning on source B, the signal processor is in a steady state. This "steady state," due to various perturbations, is subject to perturbation by source B as soon as it is turned on. Like an oscillator, this perturbation, however small it may be initially, will gradually set off a chain reaction and shift the steady state operating point to that dictated by the simultaneous presence of both sources A and B. The apparent initial non-response to source B is due to the assumption of a perfect null in the beam pattern directed toward source A and a perfect correlator in the form of the first mixer and the subsequent narrow band filter. Hence this is an inherently unstable situation. If, due to perturbations, an infinitesimal amount of energy from source B is present in the processor output, one can demonstrate readily that the end result must be a change in the operating point, namely, the λ_1 and x_i's assume the values dictated by the presence of both sources. This reasoning is in accordance with the basis which governs the numerical iterative method of obtaining the dominant characteristic value[8].

It would be remiss not to add remarks about the array factor, F. This is a mathematical expression and not the response of the SPI signal processing array. In normal arrays, the array response, or radiation pattern, is synonymous with the pattern factor, F. In a signal processing (or other adaptive) array, the array does not have a fixed response pattern. Rather, the behavior of the array is determined by the input covariance matrix. In our discussion, we have only used the pattern factor F to facilitate interpretation of the operating behavior.

V. SIMULATION EXPERIMENT

The experimental portion of this program consists of developing and using a simulator to evaluate the performance of a four-element linear array. Various parts of the experimental program are described in the following sections.
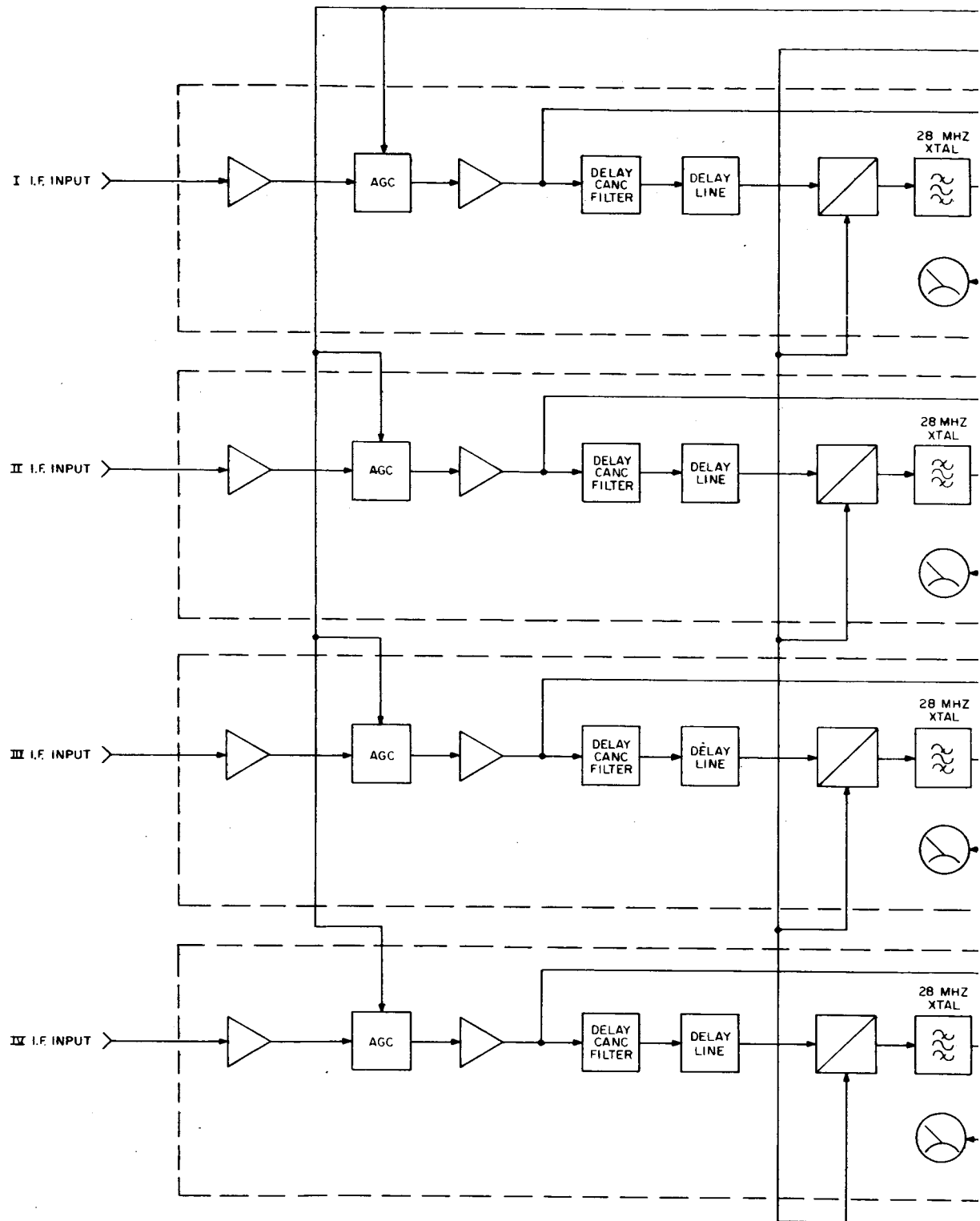
A. Signal Processor and Simulator

The signal processor is a four-channel, ratio-squared pre-detection combiner unit designed for use in the IF segment of the communication systems. Its design is similar to the two-channel predetection combiner described in Reference [1]. The four-channel signal processor permits operation on signals having a center (IF) frequency of 70 MHz and with a bandwidth of 14 MHz. The unit will accept input signal level as low as -65 dbm.

The frequency responses of the individual channels are flat to within ±0.5 db over the 14-MHz bandwidth. The AGC amplifiers are identical in gain characteristics to within about ±1 db of each other over an input dynamic range of over 30 db. A simplified block diagram of the four-channel signal processor is shown in Figure 4. The design of the combiner shown in Figure 4 differs from the functional block diagram in Figure 1 in that the AGC function in the latter is contained within the regenerative loop. The two AGC methods are functionally equivalent [1].

The signal processor has monitors which indicate the levels from each channel, i.e. the relative magnitudes of channel weighting functions, $|x_i|$. A monitor is also provided for the level of the processor output. The monitors therefore provide visual indicators of the behavior of the processor.

The simulator is designed to produce four test signals, one for each input of the four-channel signal processor. The four test signals represent output from antennas in a four-element linear array which is illuminated by an extended source (background noise), a fixed point source

I I.F. INPUT

AGC

DELAY CANC FILTER

DELAY LINE

28 MHZ XTAL

II I.F. INPUT

AGC

DELAY CANC FILTER

DELAY LINE

28 MHZ XTAL

III I.F. INPUT

AGC

DELAY CANC FILTER

DELAY LINE

28 MHZ XTAL

IV I.F. INPUT

AGC

DELAY CANC FILTER

DELAY LINE

28 MHZ XTAL

26A
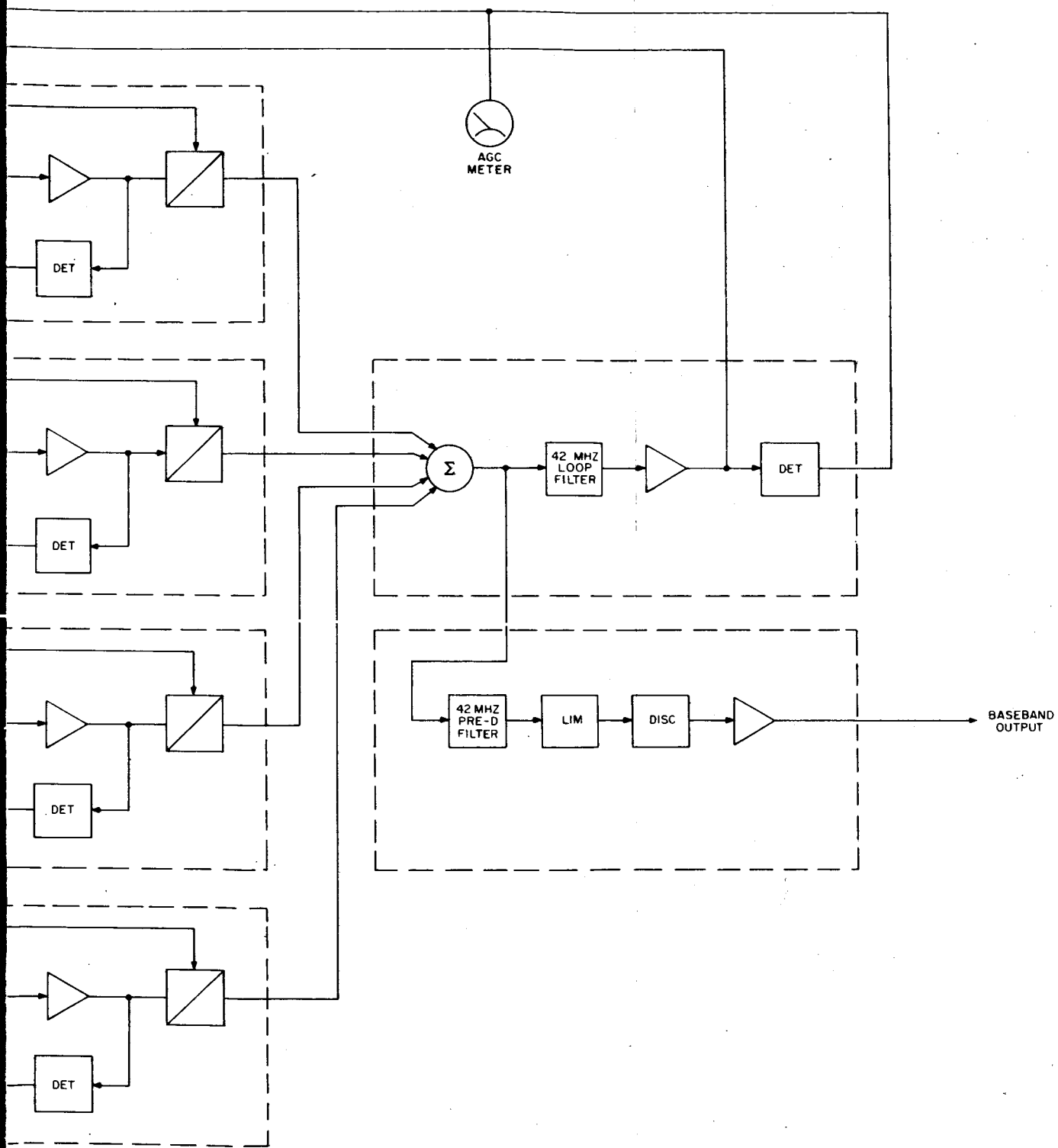
Figure 4.   Four-Channel SPI Predetection
Combiner - Block Diagram

27

(interference or noise) and a movable point source (desired signal). The electromagnetic environment simulated is illustrated in Figure 5.

The simulator generates the test signals by the method shown in Figure 6. The simulator starts with a movable point source signal which is phase-shifted through three series phase-shifters, each capable of variable phase-shift from -180° to +180°. Four tapped outputs represent the signals as received by the antenna elements. The phase-shifters effectively simulate the spatial retardation phase. The phase-shifted desired signals (from the movable source) are applied to separate summers for mixing with the partially coherent interference or noise signals prior to application to the signal processor. For simulating a discrete interference or noise source at zenith, a second signal generator is applied to all four summers without phase-shifting. The partially coherent noise or interference signal to the summers is obtained by weighting (or mixing) outputs of four independent noise generators (see Appendix).

The phase-shifters in Figure 6 are voltage adjustable to simulate different positions of the movable point source. The effective size of the extended source is varied by changing the rules of mixing the independent noise sources and is accomplished by one of many resistive matrix plug-in networks.

The simulator is tested for phase accuracy. For example, the fixed point source (representing discrete noise or interference source) is applied alone to the simulator and the phases of the simulator outputs measured to see if they are identical (for zenith direction). The phases are measured to an accuracy of ±5°.

B.   Results

A computer program has been devised to calculate the theoretical and compare with the measured signal processing gain of a four-channel SPI signal processing antenna array. The computation assumes a linear array. This leads to (see Eq. (26)) . . .
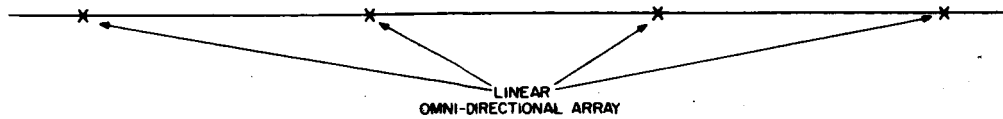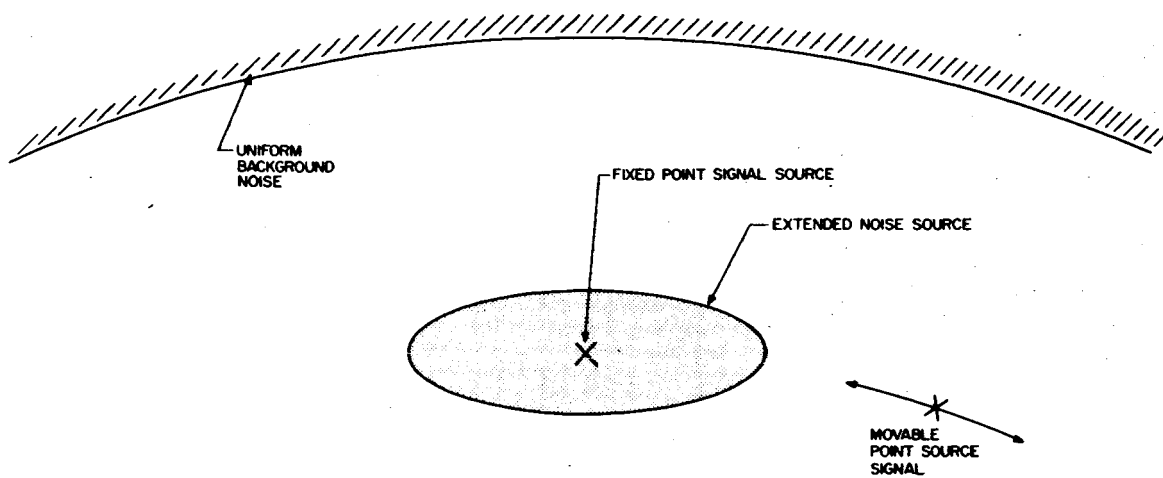
UNIFORM
BACKGROUND
NOISE

FIXED POINT SIGNAL SOURCE

EXTENDED NOISE SOURCE

MOVABLE
POINT SOURCE
SIGNAL

LINEAR
OMNI-DIRECTIONAL ARRAY

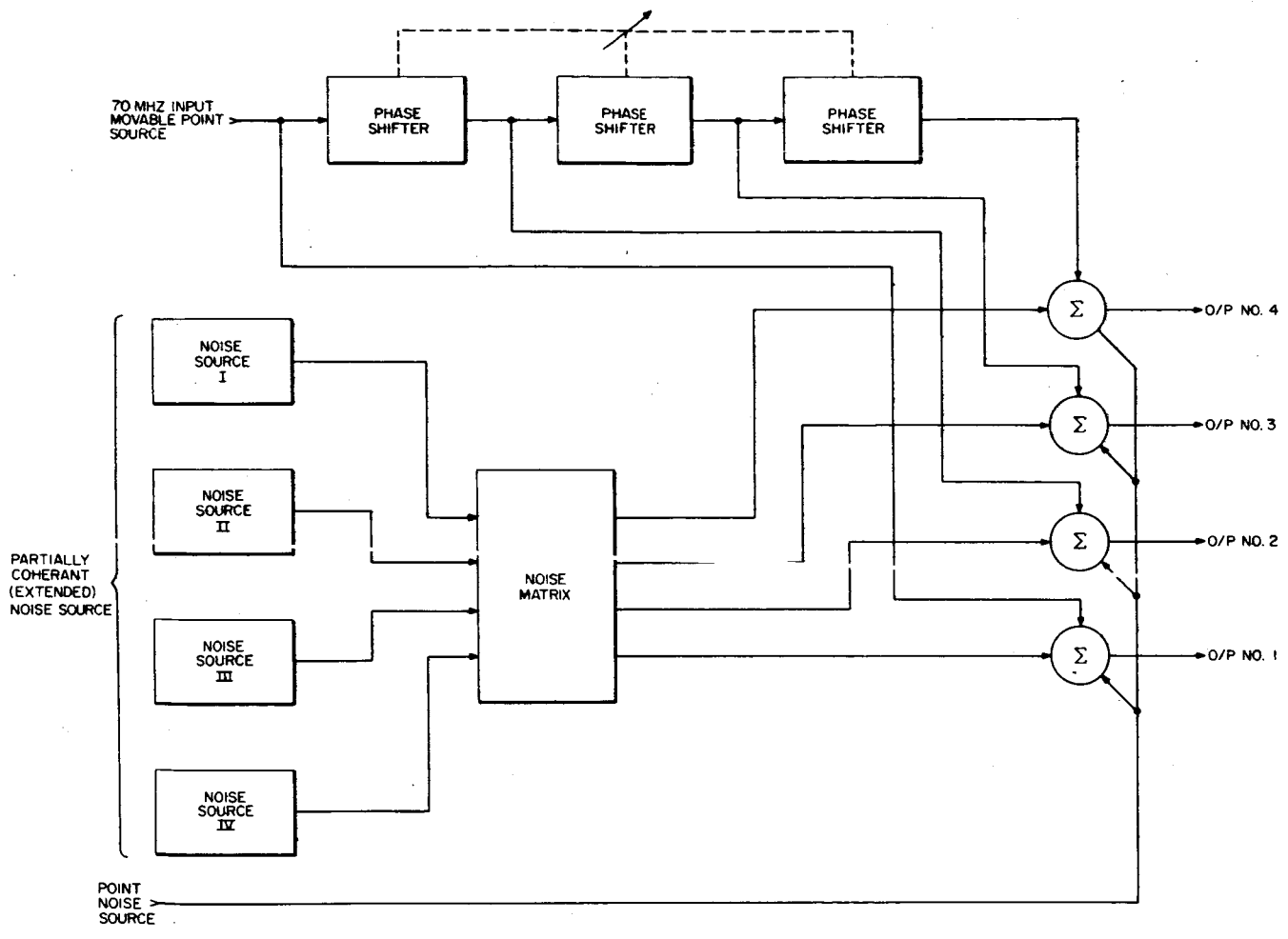Figure 5.   Antenna/Signal System to be Simulated

Figure 6.   Simulator Block Diagram

30

$$\delta_{ik} = (i-k)2\pi d \qquad\qquad (66)$$

where d is the longitudinal separation between adjacent array elements in fractions of a wavelength. For two sources in different directions, δ further represents the differential longitudinal separation for the two sources.

With the array elements restricted to N = 4, the variables for computations are:

$$w, \quad d, \quad \text{and} \quad \frac{\sigma_s^2}{\sigma_n^2}$$

where
$$w = \frac{\pi \beta \ell \cos \theta_n}{\lambda_o} \qquad\qquad (67)$$

(The coherence coefficient for the ith and k^{th} elements is thus, from Eq. (23),

$$v_{ik} = \text{sinc}[w(i-k)] \quad).$$

The computer program is straightforward in that it evaluates, for each set of input variables; the dominant eigenvalue from the characteristic function in Eq. 30, the associated eigenvector $X = \{x_1, x_2, x_3, x_4\}$, and the corresponding signal processing gain defined in Eq. (49). In the following, the (signal) processing gain so calculated is shown for various combinations of the input variables.

Figures 7 through 9 show the processing gain as a function of longitudinal separation, δ, for input signal-to-noise ratio $\frac{\sigma_s^2}{\sigma_n^2} = 0.1, 1,$ and 10 respectively. For each input signal-to-noise ratio, the processing gain versus longitudinal separation is shown with w as a parameter. For convenience, we may refer to w as the incoherence parameter, i.e. large w means greater incoherence or decorrelation.

The calculated results indicate that, for large value of incoherence parameter w, the four-element array is essentially non-directive
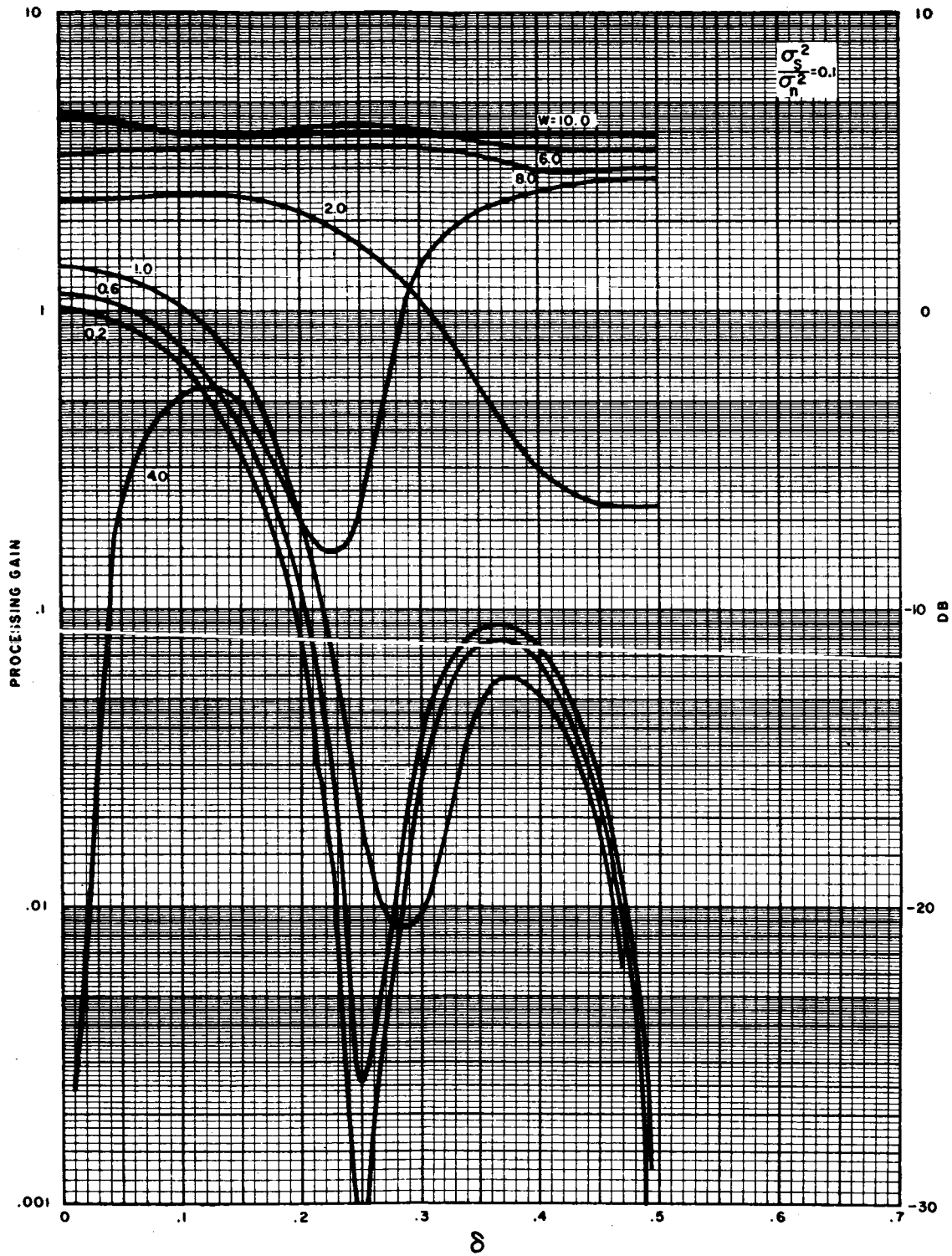
Figure 7. Processing Gain vs Longitudinal Separation for $\dfrac{\sigma_s^2}{\sigma_n^2} = 0.1$
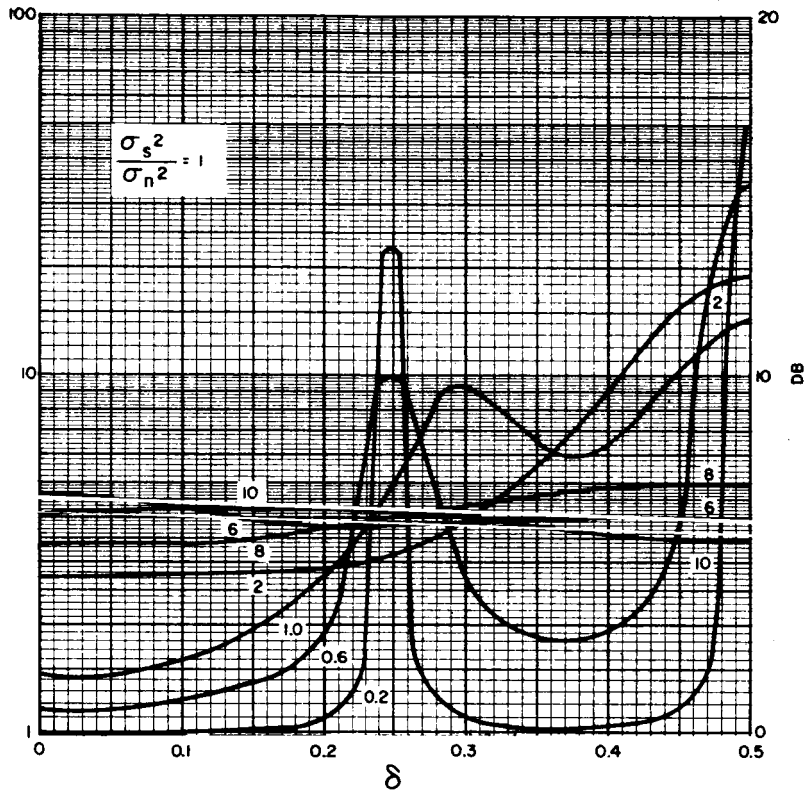
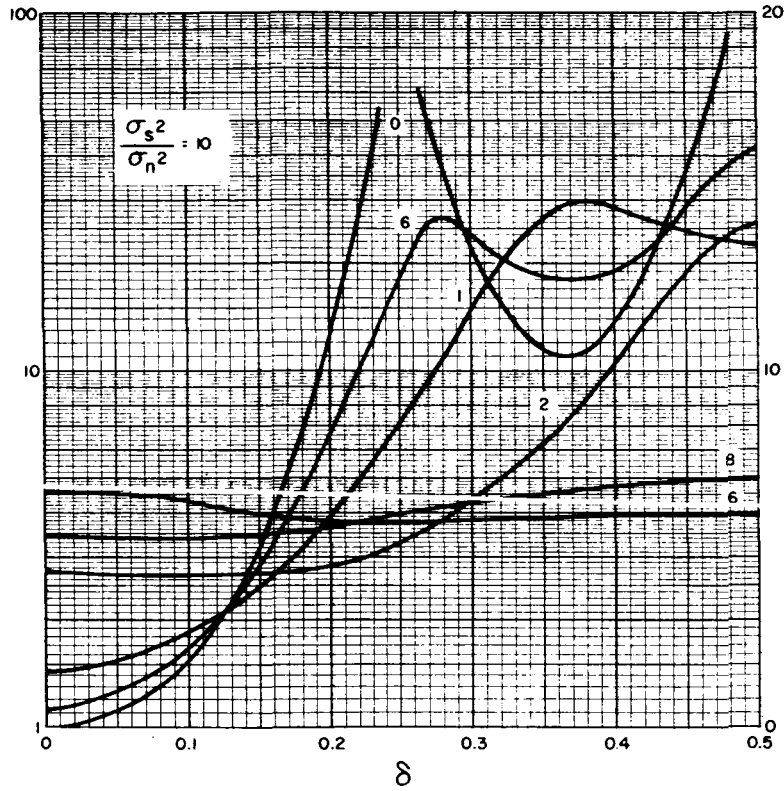Figure 8. Processing Gain vs Longitudinal Separation for $\dfrac{\sigma_s^2}{\sigma_n^2} = 1.0$

Figure 9.   Processing Gain vs Longitudinal Separation for $\dfrac{\sigma_s^{\,2}}{\sigma_n^{\,2}} = 10$

and posesses a signal processing gain of four, which is independent of the input signal-to-noise ratio. For small value of the incoherence parameter, a processing gain is experienced if the input signal-to-noise ratio is equal to or greater than unity, whereas the gain may become a loss (gain less than unity) if, at the input, $\frac{\sigma_s^2}{\sigma_n^2} < 1$.

For a four-element array, the normal array factor F has nulls at d = 0.25 and 0.5. At these points, the processing gain may become exceedingly large or approaches zero, depending on w and $\frac{\sigma_s^2}{\sigma_n^2}$.

A rather interesting point is shown in Figure 7 where, for $\frac{\sigma_s^2}{\sigma_n^2}$ = 0.1 and w = 4.0, an apparent minimum in processing gain is indicated for d = 0. This is due to the fact that, in the neighborhood of w = 4, the coherence coefficient is negative and with magnitude exceeding 0.1. We can look upon this as a partially coherent noise source which has a coherent component of 0.1 unit or greater in energy relative to the total noise of unity energy Since the signal power is $0.1(\frac{\sigma_s^2}{\sigma_n^2} = 0.1)$, the coherent component of noise dominates the behavior of the signal processor. Since the coherent noise component has negative correlation, the net result is a set of weighting functions x_i's which tend to yield little or no signal at the output of the processor. This phenomenon is more readily illustrated by the curves in Figure 10 and 11 where, for d = 0 and 0.25 respectively, the processing gain is shown as a function of w with $\frac{\sigma_s^2}{\sigma_n^2}$ as a parameter. Note that for $\frac{\sigma_s^2}{\sigma_n^2} \geq .2$ the null in the signal processing gain near w = 4 disappears. Figures 10 and 11 clearly indicate that, for large w, the processing gain approaches 4 (or 6) db.

For w >> 1, we expect the measured processing gain to be 4 ($\approx$ 6 db). This is indeed the case as shown in Figure 12 for $\sigma_s^2 \geq \sigma_n^2$. The reduction in processing gain for weak signal, i.e. $\sigma_s^2 < \sigma_n^2$ is not in accordance with prediction. This departure from ideal performance is not well understood but is believed to be caused largely by the narrow band crystal filters at 28 MHz which do not have adequate selectivity. That is, the integration time is too short. Other plausible causes for the departure include the non-ideal characteristics of the mixers which may tend to suppress weak signals.
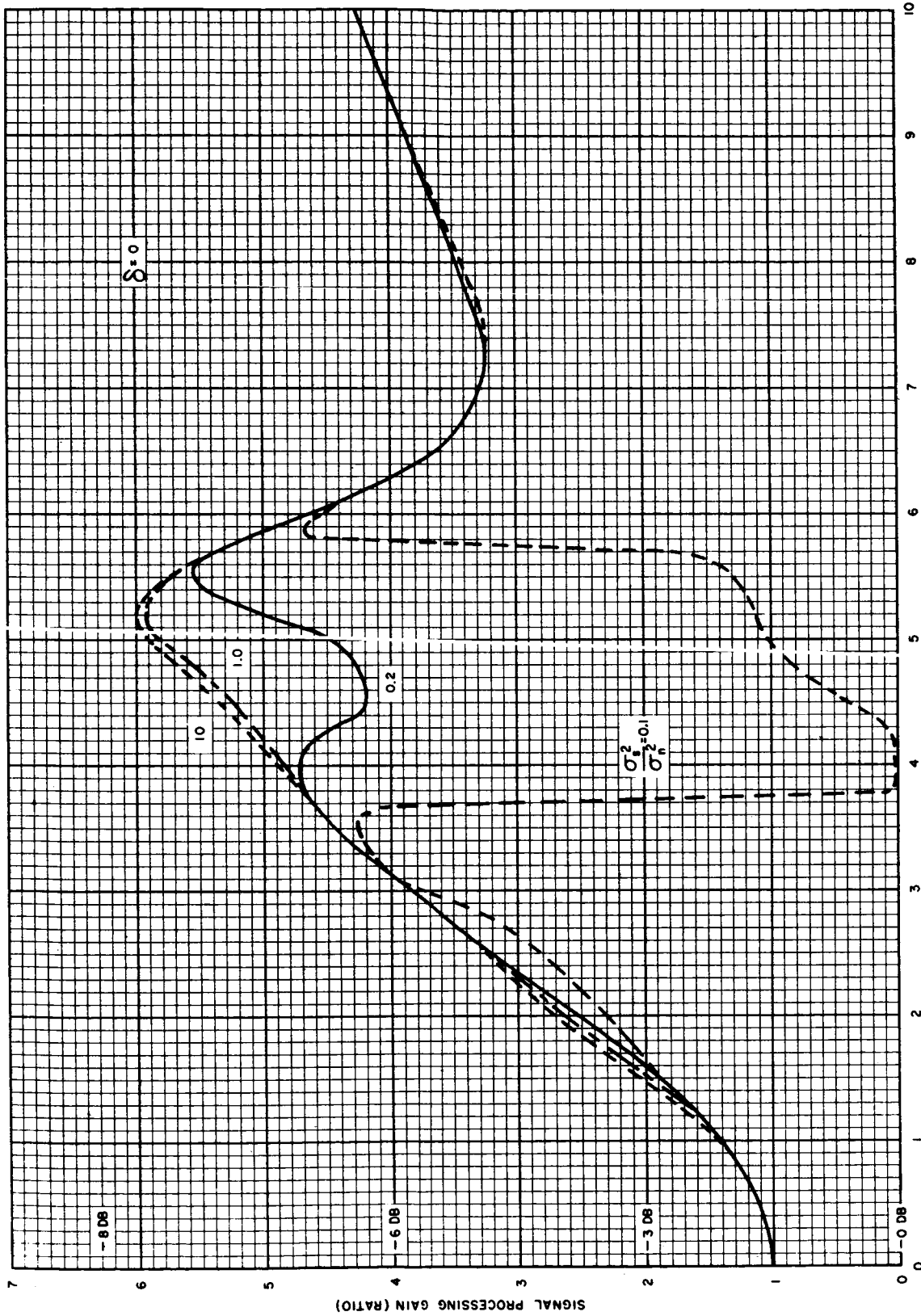
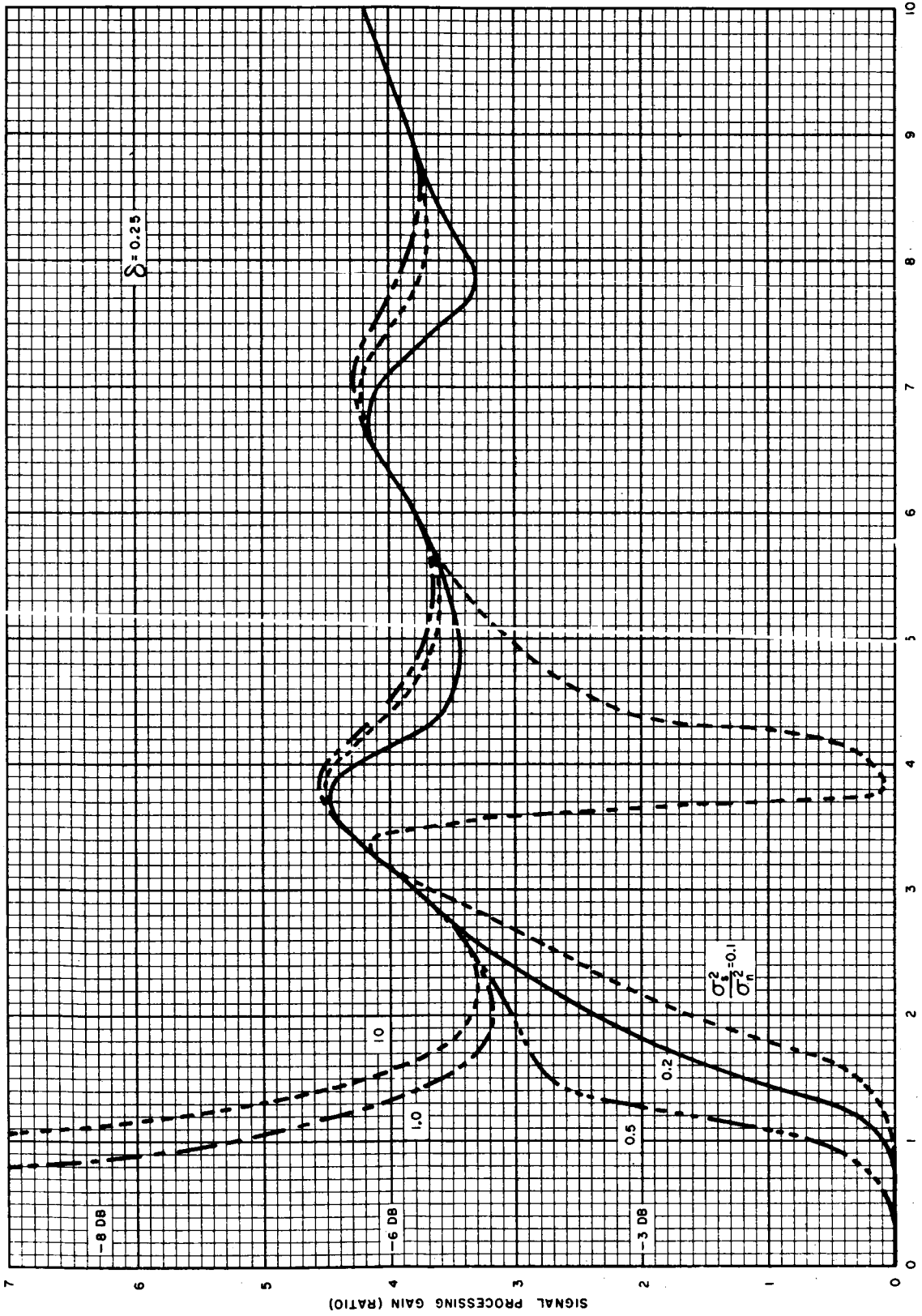Figure 10.   Processing Gain vs Incoherence Parameter for $\delta = 0$

Figure 11. Processing Gain vs Incoherence Parameter for $\delta = 0.25$
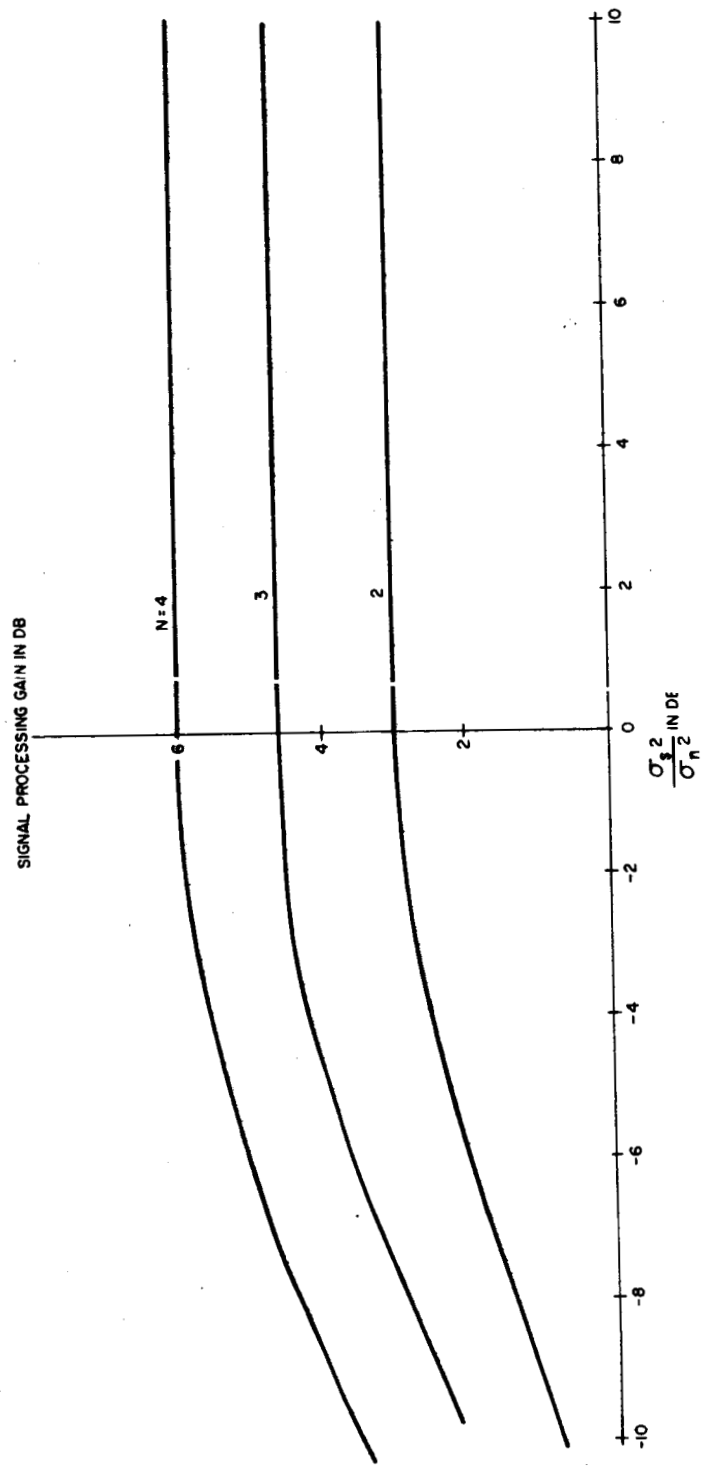
37

Figure 12. Processing Gain for Uncorrelated Input Noises

Figure 13 shows the measured signal processing gain for w = 0, i.e. coherent noise source, for $\frac{\sigma_s^2}{\sigma_n^2}$ = 2 and 10. The measured data are in good agreement with the calculated data, especially in demonstrating the maxima at δ = . 25 and . 50 where the four-element array has null in its array factor. The comparison of experimental and theoretical data suggests that the experimental signal-to-noise ratios ($\frac{\sigma_s^2}{\sigma_n^2}$) may be actually higher than indicated. Such errors are inherent in the instrument used to make noise measurement.

In Figure 14, theoretical and experimental data are shown for partially coherent noise; the processing gain is given as a function of δ for $\frac{\sigma_s^2}{\sigma_n^2}$ of 10 (= 10 db), and for w = 0.6 and 2.0. The experimental data deviated considerably from the theoretical data. However, the general trend of the predicted behavior of the processor is well verified by measured data. In the present case of simulating partially coherent illumination, the discrepancy between the measured and the theoretical data is quite possibly due to residual phase shifts in the matrix network of the simulator which combines independent noise sources. Unintentional phase shift tends to degrade the ability of the signal processor to provide the predicted gain much as the problem of achieving good side lobe level in a conventional array when phasing is inaccurate.

In spite of the difficulties encountered in the simulation experiment, we have demonstrated the most important aspect of the processor. That is, the signal processor exhibit array response which is totally dependent on the array configuration and the direction, number, and the angular sizes of the sources. Furthermore, it has also been demonstrated that the processing gain is achieved for a signal which is stronger than the interference (or noise).
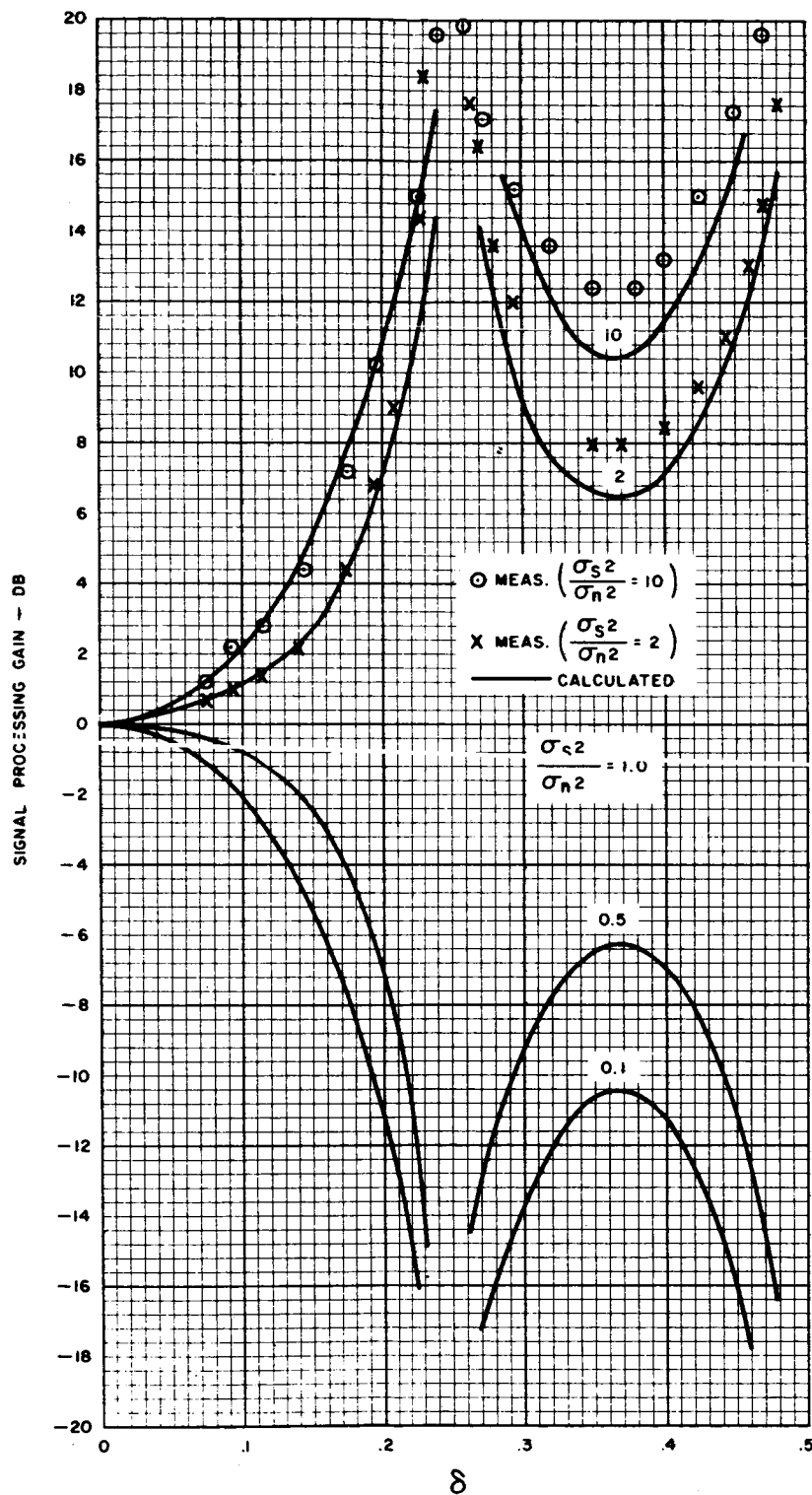
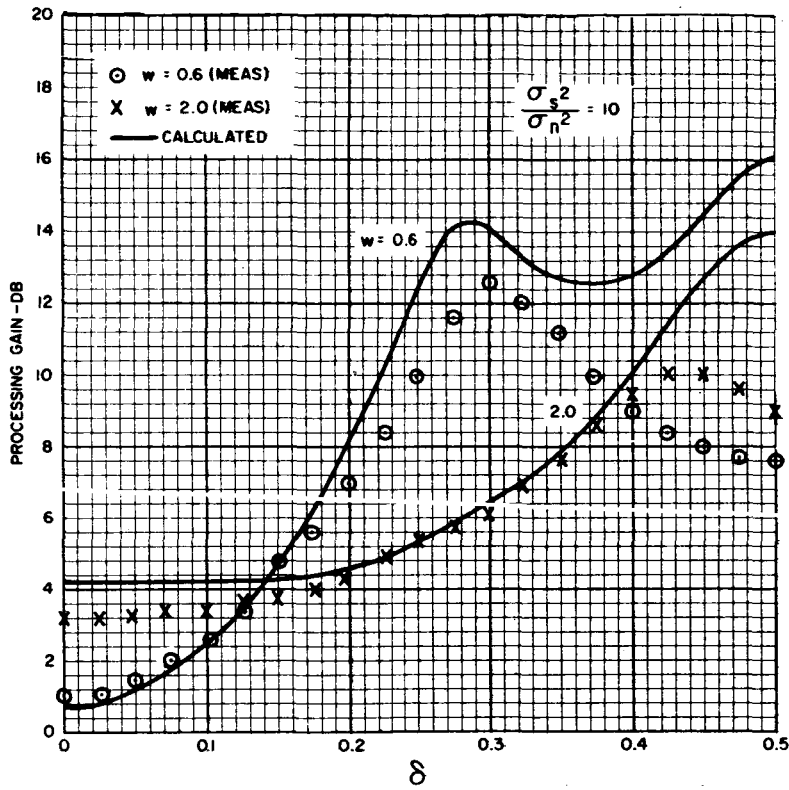Figure 13. Experimental Results - Processing Gain for w = 0

Figure 14. Experimental Results - Processing Gain for $\dfrac{\sigma_s^2}{\sigma_n^2}$

VI.   CONCLUSIONS AND RECOMMENDATIONS

A.   Summary

The study of a multi-channel signal data processor when the system is coupled to a multi-element array for receiving radio frequency signals has been directed toward the further understanding of processing of signals from antenna elements by the Raytheon Synthetic Phase Isolation technique. The antenna systems must cope with many undesired signals as well as the prime transmissions. Space communication antennas must contend with sky noise, the influence of distributed sources such as the larger natural sources and the more uniformly distributed background noise. The receiving array employing predetection combining has been carefully analyzed to determine the behavior in these environments. The results of the study can be summarized to state that the array using SPI is an adaptive phased array.

The essence of the predetection signal processing involves a regenerative configuration (or oscillator) which provides as many branches or modulator drive signals as there are elements in the array. The relative phases of these modulator drive signals modify, correspondingly, the relative phases of the received signals. For the reception of information from a single source which is coherent but for an RF phase shift, the signal processor provides the phase shift and combines the information in phase and on a ratio-squared weighting basis.

When more than one signal is present, the signal processor modifies the oscillator phases such as to achieve a maximum of received signal. Because the technique employs essentially linear signal processing techniques, a multiplicity of signals is readily handled. Given omnidirectional elements in a simple linear array, the processor will steer the "beam" to the resultant wavefront of two signals. The signals from the elements are then weighted to provide a maximum of information. The weighting for the single plane wave condition is equal weighting which, in general, does not apply in the multiple source case.

The case of uniformly distributed background noise and a
point source results in a behavior identical to the equal area, single aperture
configuration. That is, the output S/N is equal in both arrangements. Thus,
for space communications, the uniform sky noise does not change the system
whether or not the SPI predection signal processor is used. Other sources
will have an effect determined by their power and coherence over the area of
the array.

The self-steering or adaptive array employing this predetec-
tion signal processing technique has significant advantages which are achieved
within certain restrictions. Advantages include:

1. Elements of the array may be positioned independently of
the usual geometric restrictions, namely radio wavelength positioning toler-
ances.

2. The maximum of power incident upon the array aperture is
made available to the demodulation system which results in a maximum S/N
ratio for the receiving system.

3. The weighting of the inputs from the elements is ratio squared.
This results in a maximum S/N for the system, even when elements of unequal
size or of differing directivity are employed.

4. The static or quiescent condition is to form a beam much
like the conventional phased array. The weighting factors mentioned above
do result in modifiers that improve the output S/N ratio.

The prime disadvantage that the self-steering array produces
is the desire to focus on the stronger of the available signals. This, of course,
may mean the loss of a desired signal. However, it is not to be inferred that
the array factor is lost in the discrimination against "off beam" signals.

The study indicates clearly that this is a powerful signal processing technique for adaptive arrays.

B. Recommendations

The laboratory tests and analytical evaluation has shown that predetection signal processing is achievable. The tests made with an antenna simulator have provided data as to the behavior of the signal processor under simulated conditions. These checks have been used to verify the analytical predictions and within the tolerances of design the analysis has been confirmed.

With this background, the logical next step is to assemble four or more receiving elements complete with antennas and to demonstrate the performance of an adaptive array using predetection signal data processing in an experimental system. The ability to obtain full aperture gain over a wide range of geometric arrangements is an essential characteristic if very large arrays are to be practical. This is because of the mechanical tolerance restrictions. Once this has been clearly demonstrated, a new avenue is open for the construction of the large receiving apertures.

This experimentation could be coupled with investigations as to the ability to make a multi-aperture low-noise receiving configuration. Bearing in mind the objectives of extending the design to larger apertures and of achieving a multi-element phased array with a low noise temperature and very low side lobes, it appears that predetection signal processing has the capability to make significant contributions to the technology of space communications.

44

VII.   ACKNOWLEDGEMENT

VIII. <u>REFERENCES</u>

[1]   Bickford, W. J., R. G. Cease, D. B. Cooper and H. J. Rowland, "Study of a Signal Processor Employing a Synthetic Phase Isolator," Technical Report CDP-TR-2, Raytheon Company, CADPO, Contract No. NAS 12-82, October 1966.

[2]   Brennan, D. G., "Linear Diversity Combining Techniques," Proc. IRE, Vol. 47, pp. 1075-1102, June 1959.

[3]   Schwartz, M., W. R. Bennett and S. Stein, "Communication Systems and Techniques," Chapter 10, McGraw-Hill Book Company, 1966.

[4]   Guillemin, E. A., "Mathematics of Circuit Analysis," The Technology Press, John Wiley & Son, Inc., Chapter III, 1949.

[5]   Beran, M. and G. B. Perrant, "Theory of Partial Coherence," Prentice Hall, 1964.

[6]   Poirier, J. L. and F. J. Zucker, "Partial Coherence, a Nonstatistical Approach and Some Basic Microwave Experiments," IEEE Trans. on Ant. and Prop., Vol. AP-15, No. 1, pp. 4-9, January 1967.

[7]   Courant, R. and D. Hilbert, "Methods of Mathematical Physics," Vol. 1, Chapter 1, Interscience Publishers, Inc., 1953.

[8]   Hildebrand, F. B., "Methods of Applied Mathematics," Chapter 1, Prentice Hall, 1965.

APPENDIX

Simulation of Partially Coherent Noise

Laboratory evaluation of the multi-channel SPI signal processor without the use of large antennas can be performed by simulating the outputs of an antenna array due to a partially coherent noise source. Several techniques can be devised to achieve the desired results, and a few of these are described briefly. A convenient method for arrays of few elements is that of linear mixing (transformation) of N independent noise sources.

Scale Model Method

A scaled-down model of the partially coherent source and the antenna array may be constructed in the laboratory. The source can be a line radiator such as a flourescent lamp. The number of pickup horns simulates the actual antenna array. The operating frequency depends on the scaling factor involved. This method is cumbersome and need not be considered further.

Delay Line Method

A narrow band noise has an autocorrelation function which is of the same functional form as the spatial coherence function if we identify the spatial separation of the coherence function with the time shift of the autocorrelation function. This suggests that a tapped delay line can be used to simulate the antenna array outputs.

For narrow band noise with low carrier frequency, multi-tapped delay lines are readily available. A sharp cut-off filter is needed

prior to the delay line. The tap spacing should be small compared with the inverse of the filter bandwidth. At high carrier frequency, say, 70 MHz, and large bandwidth, say, 10 to 20 MHz, the delay line requirements would be sufficiently severe.

Ideally, the partial coherence property can be simulated at low carrier frequency or even at baseband. These are then separately up-converted to the desired carrier frequency. In the up-conversion process, the local oscillator drives to the mixers should be phase-synchronized. Fixed phase shifts may be introduced at these points to simulate the effect of antenna phasing due to the direction of the source.

Linear Mixing Method

N antenna array outputs, n_i's, $i = 1, 2, 3, \ldots, N$, may be simulated by linear mixing of N independent noise sources, x_i's, $i = 1, 2, 3, \ldots, N$. If

$$\overline{n_i n_j} = \sigma_n^2 \gamma_{i_j}, \quad \gamma_{i_j} = \gamma_{j_i}$$

and

$$\overline{x_i x_j} = \sigma_n^2 \delta(i, j)$$

$$\begin{aligned} \delta(i, j) &= 1 \quad \text{if } i = j \\ &= 0 \quad \text{if } i \neq j \end{aligned}$$

then

$$n] = [A] \, x]$$

where $n]$ and $x]$ are column matrices for n_i's and x_i's respectively, and $[A]$ is an $N \times N$ matrix of coefficients of transformation. $[A]$ is related to the coherence matrix,

$$[\gamma] = [A] [A]_t$$

It can be shown that, since $[\gamma]$ is positive real, a diagonal form of $[A]$

can be found. The coefficients of the diagonal matrix can be determined from a set of recurrence formulas.

The coefficients $a_{i,j}$ are easily computed for any given coherence matrix. The implementation of the method requires only a resistive matrix board. For large N, this method may be unattractive in comparison with the delay line method. The N independent noise sources required for the mixing method are another disadvantage, as the delay line method needs only one noise source. However, for small N, such as N = 4 for the NASA SPI Study, the linear mixing method may be quite suitable.

The partially coherent noise waveforms n_i's are derived from the independent (incoherent) waveforms x_i's :

$$n_1 = a_{11} \ x_1$$

$$n_2 = a_{21} \ x_1 + a_{22} \ x_2$$

$$\cdots \cdots \cdots \cdots \cdots$$

$$n_i = a_{i1} \ x_1 + a_{i2} \ x_2 + \ldots + a_{ii} \ x_i$$

The coefficients a_{ij}'s are obtained from the recurrence formulas:

$$a_{11} = \gamma_{11}$$

$$a_{21} = \frac{\gamma_{21}}{a_{11}} \quad , \quad a_{22} = \sqrt{1-a_{21}^2}$$

$$a_{31} = \frac{\gamma_{31}}{a_{11}} \quad , \quad a_{32} = \frac{\gamma_{32} - a_{21} \ a_{31}}{a_{22}} \quad , \quad a_{33} = \sqrt{1 - a_{31}^2 - a_{32}^2}$$

$$\cdots \cdots \cdots \cdots \cdots \cdots \cdots \cdots \cdots \cdots$$

$$a_{i1} = \frac{\gamma_{i1}}{a_{11}}$$

$$a_{i2} = \frac{\gamma_{i2} - a_{21} a_{i1}}{a_{22}}$$

. . . .

$$a_{ij} = \gamma_{ij} - a_{j1} a_{i1} - a_{j2} a_{i2} - \ldots, - a_{j, j-1} a_{i, i-1}$$

. . . .

$$a_{ii} = \sqrt{1 - a_{i1}^2 - a_{i2}^2 - \ldots, - a_{i, i-1}^2}$$

The coefficients $a_{i,j}$ are easily computed for any given coherence matrix. The implementation of the method requires only a resistive matrix board. For large N, this method may be unattractive in comparison with the delay line method. The N independent noise sources required for the mixing method are another disadvantage, as the delay line method needs only one noise source. However, for small N, such as N = 4 for the NASA SPI Study, the linear mixing method may be quite suitable.

For the case of N = 4 (for a four-channel combiner), the mixing coefficients have been calculated and shown in Table I for various values of w. The quantity w is defined as the ratio

$$w = \frac{\pi \beta \ell \cos \theta_n}{\lambda_0}$$

where β is the angular width of the noise source, θ_n is the direction of the source measured from normal to array axis, λ_0 is the wavelength and ℓ is the array element spacing.

The coherence coefficient between two elements i and j is

$$\gamma_k = \gamma_{i-j} = \text{sinc } wk$$

For simulating four partially coherent noise sources, [n], from four

independent sources, [x], the following relation is established

$$[n] = [a][x]$$

where [a] is a 4 × 4 matrix for which coefficients to one side of the principal diagonal are zero. The remaining coefficients are tabulated in Table I for w varying from 0 to 10.0.

The particular form of transformation has its limitation. For $0 < \frac{w}{\pi} \le 0.6$, the terms of the principal diagonal may be imaginary. In other words, although the transformation is mathematically correct, the transformation is not necessarily physically realizable. The explanation of this difficulty goes as follows. The coherent matrix (N × N) is only a segment of a matrix of infinite order; hence, the transformation must be performed on that basis. This requires, therefore, an infinite number of independent noise sources. In practice, a finite number of independent noise sources is sufficient if the range of w is restricted. Thus, the numerical case involved here using only four independent sources results in the restrictions that

$$w = 0 \qquad \text{and} \qquad w > 0.6\pi$$

In the intermediate range of w, one can use an additional number of independent sources, or resort to the delay line method. Since we now need only to simulate for small values of w, the amount of delay involved becomes reasonably convenient to handle. Thus, for a noise bandwidth of about 10 MHz, a delay range of a few tenths of a microsecond will be adequate. This presumably can be obtained through the use of transmission lines.

w	r_0	r_1	r_2	r_3	a_{11}	a_{21}	a_{22}	a_{31}	a_{32}	a_{33}	a_{41}	a_{42}	a_{43}	a_{44}
0.00	1.0	1.0	1.0	1.0	1.0	1	0.0	1	0.0	0.0	1	0.0	0.0	0.0
0.10	1.0	.9999	.9993	.9985	1.0	.9999	.0141	.9993	.0496	j.0078	.9985	.0638	j.3205	j.3222
0.03	1.0	.9985	.9941	.9867	1.0	.9985	.0548	.9941	.1077	.0129	.9867	.1624	.9069	j.9068
0.1	1.0	.9836	.9355	.8584	1.0	.9836	.1804	.9355	.3514	.0368	.8584	.5055	-3.3206	j3.3192
0.3	1.0	.8584	.5046	.1093	1.0	.8584	.5129	.5046	.8290	.2411	.1093	.8009	-2.5292	j2.4595
0.4	1.0	.7567	.2338	-.2146	1.0	.7567	.6538	.2338	.8868	.3986	-.2146	.1092	1.5296	j1.1822
0.5	1.0	.6366	0.0	-.2122	1.0	.6366	.7712	0.0	.8254	.5645	-.2122	.1750	1.1103	j.5554
0.6	1.0	.5045	-.1559	-.1039	1.0	.5045	.8634	-.1559	.6754	.7208	-.1039	.1198	.5790	.7998
0.9	1.0	.1093	-.1039	.0954	1.0	.1093	.9904	-.1039	.1218	.9820	.0954	-.1154	.1155	.9819
1.0	1.0	0.0	0.0	0.0	1.0	0.0	1.0	0.0	0.0	1.0	0.0	0.0	0.0	1.0
1.5	1.0	-.2130	0.0	.0707	1.0	-.2130	.9771	0.0	-.1914	.9815	.0707	.0015	-.2173	.9729
2.0	1.0	0.0	0.0	0.0	1	0.0	1	0.0	0.0	1	0.0	0.0	0.0	1
2.5	1.0	.1273	0.0	-.0424	1.0	.1273	.9902	0.0	.1285	.9902	-.0424	.0055	.0435	.9908
3.0	1	0.0	0.0	0.0	1	0.0	1	0.0	0.0	1	0.0	0.0	0.0	1
3.5	1.0	-.0909	0.0	.0303	1.0	-.0909	.9906	0.0	-.0918	.9909	.0303	-.0028	-.0401	.9908
4.0	1	0.0	0.0	0.0	1	0.0	1	0.0	0.0	1	0.0	0.0	0.0	1
4.5	1.0	.0707	0.0	-.0236	1.0	.0707	.9907	0.0	.0714	.9907	-.0236	.0017	-.0239	.9909
5.0	1	0.0	0.0	0.0	1	0.0	1	0.0	0.0	1	0.0	0.0	0.0	1
5.5	1.0	-.0579	0.0	.0193	1.0	-.0579	.9908	0.0	-.0584	.9908	.0193	.0011	.0196	.9909
6.0	1	0.0	0.0	0.0	1	0.0	1	0.0	0.0	1	0.0	0.0	0.0	1
6.5	1.0	.0490	0.0	.0163	1.0	.0490	.9909	0.0	.0494	.9909	-.0163	.0008	-.0164	.9909
7.0	1	0.0	0.0	0.0	1	0.0	1	0.0	0.0	1	0.0	0.0	0.0	1
7.5	1.0	-.0424	0.0	.0141	1.0	-.0424	.9909	0.0	-.0427	.9908	.0141	.0006	.0142	.9910
8.0	1	0.0	0.0	0.0	1	0.0	1	0.0	0.0	1	0.0	0.0	0.0	1
8.5	1.0	.0374	0.0	-.0125	1.0	.0374	.9909	0.0	.0377	.9908	-.0125	.0004	-.0126	.9910
9.0	1	0.0	0.0	0.0	1	0.0	1	0.0	0.0	1	0.0	0.0	0.0	1
9.5	1.0	-.0335	0.0	.0112	1.0	-.0335	.9909	0.0	-.0338	.9909	-.0112	.0004	.0113	.9910
10.0	1	0.0	0.0	0.0	1	0.0	1	0.0	0.0	1	0.0	0.0	0.0	1

Table I.   Transformation Coefficients